

Black Hole Mergers From Globular Clusters Observable by LISA I: Eccentric Sources Originating From Relativistic N -body Dynamics

Johan Samsing^{1,★}, Daniel J. D’Orazio²

¹Department of Astrophysical Sciences, Princeton University, Peyton Hall, 4 Ivy Lane, Princeton, NJ 08544, USA

²Department of Astronomy, Harvard University, 60 Garden Street Cambridge, MA 01238, USA

Accepted XXX. Received YYY; in original form ZZZ

ABSTRACT

We show that nearly half of all binary black hole (BBH) mergers dynamically assembled in globular clusters have measurable eccentricities ($e > 0.01$) in the LISA band (10^{-2} Hz), when General Relativistic corrections are properly included in the N -body evolution. If only Newtonian gravity is included, the derived fraction of eccentric LISA sources is significantly lower, which explains why recent studies all have greatly underestimated this fraction. Our findings have major implications for how to observationally distinguish between BBH formation channels using eccentricity with LISA, which is one of the key science goals of the mission. We illustrate that the relatively large population of eccentric LISA sources reported here originates from BBHs that merge between hardening binary-single interactions inside their globular cluster. These results indicate a bright future for using LISA to probe the origin of BBH mergers.

Key words: gravitation – gravitational waves – stars: black holes – stars: kinematics and dynamics – globular clusters: general

1 INTRODUCTION

Gravitational waves (GWs) from merging binary black holes (BBHs) have been observed (Abbott et al. 2016b,c,a, 2017a,b); however with the sparse sample collected to far, it is not clear where and how these BBHs formed in our Universe. From a theoretical perspective, several formation channels have been suggested including isolated field binaries (Dominik et al. 2012, 2013, 2015; Belczynski et al. 2016b,a), dense stellar clusters (Portegies Zwart & McMillan 2000; Banerjee et al. 2010; Tanikawa 2013; Bae et al. 2014; Rodriguez et al. 2015, 2016a,b,b; Askar et al. 2017; Park et al. 2017), single-single GW captures of primordial BHs (Bird et al. 2016; Cholis et al. 2016; Sasaki et al. 2016; Carr et al. 2016), active galactic nuclei discs (Bartos et al. 2017; Stone et al. 2017; McKernan et al. 2017), galactic nuclei (O’Leary et al. 2009; Hong & Lee 2015; VanLandingham et al. 2016; Antonini & Rasio 2016; Hoang et al. 2017), and very massive stellar mergers (Loeb 2016; Woosley 2016; Janiuk et al. 2017; D’Orazio & Loeb 2017). Although these proposed pathways seem to give rise to similar merger rates and observables, recent work interestingly suggests that careful measurements of the BBH orbital eccentricity and relative spins might be the key to disentangling them. For example, BBH mergers forming as a result of field binary evolution are likely to have correlated spin orientations, except if a third object is bound and the three objects form a hierarchical triple

(e.g., Liu & Lai 2017; Antonini et al. 2017), whereas BBH mergers forming in clusters are expected to have randomized orientations due to frequent exchanges (e.g., Rodriguez et al. 2016c). However, observations so far do favor merging BHs with low spin, which naturally complicates the otherwise promising use of spin correlations. Regarding eccentricity, it was recently shown by Samsing (2017) that $\approx 5\%$ of all BBH mergers forming in globular clusters (GCs) are likely to have a notable eccentricity (> 0.1) when entering the observable range of the ‘Laser Interferometer Gravitational-Wave Observatory’ (LIGO). As argued by Samsing (2017), this population originates from GW capture mergers forming in chaotic three-body interactions (e.g., Gültekin et al. 2006; Samsing et al. 2014) during classical hardening, which explains why all recent Newtonian N -body studies have failed in resolving the correct fraction. In fact, it was analytically derived in Samsing (2017) that a Newtonian N -body code will always result in a rate of eccentric mergers that is ≈ 100 times lower compared to the (correct) General Relativistic (GR) prediction. These results were recently confirmed by Rodriguez et al. (2017) and Samsing et al. (2018c), using data from simulated GCs. As isolated BBH mergers forming in the field are expected to be circular when entering the LIGO band, these studies show that eccentricity could play a key role in distinguishing formation channels from each other.

In this paper we study how BBH mergers that form dynamically in GCs distribute and evolve in the sensitivity band of the proposed ‘Laser Interferometer Space Antenna’ mission (LISA; Amaro-Seoane et al. 2017), when GR effects are included in the dy-

* jsamsing@princeton.edu; daniel.dorazio@cfa.harvard.edu

namical modeling. Dissipative effects, such as GW emission, which usually are modeled using the post-Newtonian (PN) formalism (e.g., [Blanchet 2014](#)), have previously been shown to play a crucial role in resolving eccentric LIGO populations (e.g., [Samsing et al. 2018b](#)); however, the possible effects related to LISA have not yet been properly studied. Our motivation is to explore what can be learned about where and how BBH mergers form in our Universe from a LISA mission; we identify possible observable differences between different BBH populations formed in GCs compared to those formed in the field. Motivated by previous studies, we focus in this paper on the eccentricity distribution. We note that the recent work by [Breivik et al. \(2016\)](#) did indeed look into this; however, the data used for that study did not include GR effects, which we in this paper show are extremely important.

Using a semi-analytical approach, we find that ≈ 4 times more BBH mergers will appear eccentric (> 0.01) in the LISA band (10^{-2} Hz) compared to the results reported by [Breivik et al. \(2016\)](#), when GR effects are included. This leads to the exciting conclusion that about 40% of all GC BBH mergers are expected to have a measurable eccentricity in the LISA band, whereas a field BBH population in comparison will have $\approx 0\%$. As we describe, the merger population that leads to this increase in eccentric LISA sources, originates from BBHs that merge *between* their hardening binary-single interactions inside their GC (e.g., [Rodriguez et al. 2017](#)). This population was not included in the recent study by [Samsing et al. \(2018a\)](#), which focused solely on the BBH mergers forming *during* the binary-single interactions. These BBH mergers were shown to elude the LISA band, and joint observations with LIGO are therefore necessary to tell their GC origin. The fact that BBH mergers can be jointly observed by LISA and LIGO was recently pointed out by [Sesana \(2016\)](#) and [Seto \(2016\)](#). Discussions on BBH merger channels and eccentricity distributions relevant for LISA were presented in [Nishizawa et al. \(2016\)](#) and ([Nishizawa et al. 2017](#)). However, we note again that all previous studies have greatly underestimated the fraction of eccentric LISA sources from GCs, mainly due to the omitted GR effects in the data set derived in [Rodriguez et al. \(2016a\)](#). It would be interesting to see how the results presented in this paper affect those previous studies.

The paper is organized as follows. In Section 2 we describe the approach we use for modeling the dynamical evolution of BBHs inside GCs and their path towards merger, when GR effects are included in the problem. Our main results are discussed in Section 3, where we show for the first time that, with the inclusion of GR effects, nearly half of all BBH mergers forming in GCs are expected to be eccentric in LISA. We conclude our study in Section 4.

2 BLACK HOLE DYNAMICS IN GLOBULAR CLUSTERS

In this section we describe the new approach we use in this paper for estimating the distribution of GW frequency, f_{GW} , and eccentricity, e , of BBH mergers forming in globular clusters (GCs). Using this, we explore the possible observable differences between different BBH populations forming in GCs and those forming in the field for an instrument similar to LISA, and the role of GR in that modeling. As described in the Introduction, in the recent work by [Breivik et al. \(2016\)](#) it was claimed that $\approx 10\%$ of the GC mergers will have an eccentricity > 0.01 at 10^{-2} Hz, compared to $\approx 0\%$ for the field population. However, the simulations used in [Breivik et al. \(2016\)](#) did not treat the relativistic evolution of BBHs inside the GC correctly, which essentially prevented BBHs to merge inside their GCs (see [Rodriguez et al. \(2017\)](#) for a description). To improve on

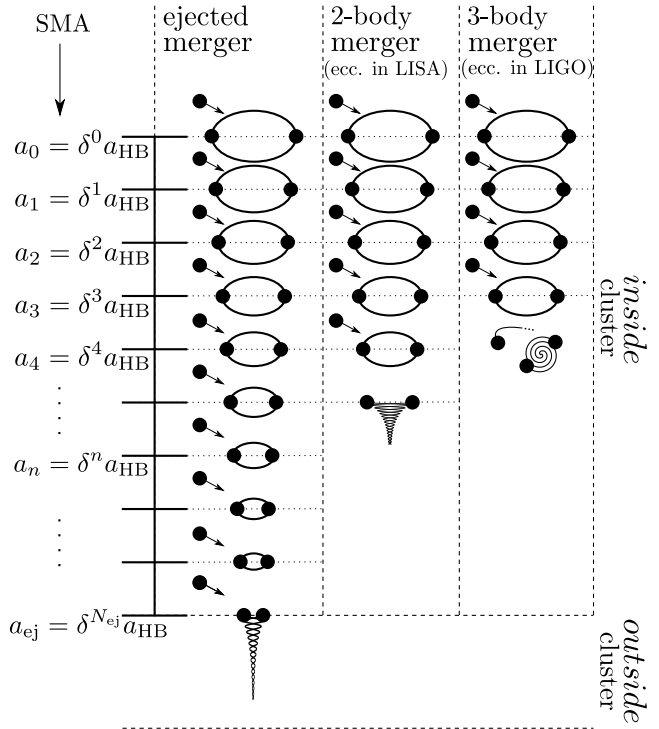


Figure 1. The graphics in the three columns above illustrate the three different dynamical pathways for merging BBHs to form, each of which result in a different type of GW merger. The horizontal steps from top to bottom illustrate the stepwise decrease in the BBH’s SMA due to hardening binary-single interactions, which progresses as $\delta^0 a_{\text{HB}}$, $\delta^1 a_{\text{HB}}$, ..., until a merger or an ejection takes place. The illustration complements the description of our model from Section 2. In short, our model assumes the BBH in question starts with an SMA = a_{HB} , after which it hardens through binary-single interactions, each of which leads to a decrease in its SMA from a to δa . This hardening continues until the SMA reaches a_{ej} , below which the BBH will be ejected from the GC through three-body recoil. If the BBH merges outside the GC within a Hubble time, we label it an ‘ejected merger’ (left column). The ejected merger progenitors form via interactions involving Newtonian gravity alone; however, when GR effects are included, the BBH can also merge inside the cluster, before ejection takes place (e.g. [Samsing 2017; Rodriguez et al. 2017](#)). This can happen either *between* or *during* its hardening interactions, outcomes we refer to as a ‘2-body merger’ (middle column) and a ‘3-body merger’ (right column), respectively. All previous studies on the eccentricity distribution of LISA sources have only considered the ‘ejected mergers’; however, as we show in this paper, the ‘2-body mergers’ clearly dominate the eccentric population observable by LISA ($e > 0.01$ at 10^{-2} Hz). In comparison, the ‘3-body mergers’ dominate the eccentric population observable by LIGO ($e > 0.1$ at 10 Hz).

their study we combine in the sections below a simple Monte Carlo (MC) method with the analytical framework from [Samsing \(2017\)](#) to estimate what the actual BBH eccentricity distribution is expected to be in the LISA band, taking into account that BBHs can form both during and between hardening binary-single interactions (e.g., [Rodriguez et al. 2017](#)). Although our approach is highly simplified, we do clearly find that GR effects play a central role in such a study. Figure 1 schematically illustrates our dynamical model described below.

2.1 Binary Black Holes Interacting in Clusters

We assume that the dynamical history of a BBH in a GC from its formation to final merger follows the idealized model described in

[Samsing \(2017\)](#), in which it first forms dynamically at the hard-binary (HB) limit (e.g., [Heggie 1975](#); [Aarseth & Heggie 1976](#); [Hut & Bahcall 1983](#)), after which it hardens through equal mass three-body interactions. Each interaction leads to a fixed decrease in its semi-major axis (SMA) from a to δa , where the average value of δ is 7/9 using the distributions from [Heggie \(1975\)](#), as shown by [Samsing \(2017\)](#). For simplicity we will use this value of δ for our modeling. The BBH will harden in this way until it either merges inside the GC, or its three-body recoil velocity exceeds the escape velocity of the GC, v_{esc} , after which it escapes. In this model, such an ‘ejection’ can only happen if the SMA of the BBH is below the following characteristic value ([Samsing 2017](#)),

$$a_{\text{ej}} \approx \frac{1}{6} \left(\frac{1}{\delta} - 1 \right) \frac{Gm}{v_{\text{esc}}^2}, \quad (1)$$

where m is the mass of one of the three interacting (assumed equal mass) BHs. The mergers that are normally considered, using Newtonian prescriptions, are the BBHs that will merge *outside* the GC, i.e. the subset of the ejected BBHs that has a GW lifetime that is less than the Hubble time, t_{H} . However, when GR effects are included, a BBH can also merge *inside* the GC in at least two different ways (e.g., [Samsing 2017](#); [Rodriguez et al. 2017](#)): The first way is *between* its hardening binary-single interactions – a merger type we will refer to in short as a ‘2-body merger’ (2b). A BBH will undergo such a merger if its GW lifetime is shorter than the time it takes for the next interaction to occur. The second way is *during* its hardening binary-single interactions – a merger type we will refer to in short as a ‘3-body merger’ (3b). Such a merger occurs if two of the three interacting BHs undergo a two-body GW capture merger during the chaotic evolution of the three-body system ([Gültekin et al. 2006](#); [Samsing et al. 2014](#)).

These three different types of mergers (ejected merger, 2-body merger, and 3-body merger) arise, as described, from different mechanisms that each have their own characteristic time scale (Hubble time, binary-single encounter time, three-body orbital time), which explains why they give rise to different distributions in GW frequency and eccentricity, as will be shown in Section 3. Below we describe how we construct these distributions from our simple model.

2.2 Deriving Eccentricity and GW Frequency Distributions

We start by considering two BHs each with mass m , in a binary with SMA equal to their HB value given by (e.g., [Hut & Bahcall 1983](#)),

$$a_{\text{HB}} \approx \frac{3}{2} \frac{Gm}{v_{\text{dis}}^2}, \quad (2)$$

where v_{dis} is the velocity dispersion of the interacting BHs. As described in Section 2.1, we assume that the dynamical evolution of this BBH is governed by isolated binary-single interactions that lead to a stepwise decrease in its SMA as follows, $\delta^0 a_{\text{HB}}, \delta^1 a_{\text{HB}}, \delta^2 a_{\text{HB}}, \dots, \delta^n a_{\text{HB}}, \dots$, until $\delta^{N_{\text{ej}}} a_{\text{HB}} \approx a_{\text{ej}}$, where n is the n ’th binary-single interaction, and N_{ej} is the number of interactions it takes to bring the BBH to its ejection value, $N_{\text{ej}} \approx \ln(a_{\text{HB}}/a_{\text{ej}})/(1 - \delta) \approx 15$ ([Samsing 2017](#)). For deriving the BBH merger fractions, GW frequencies, and eccentricity distributions, we perform the following calculations at each interaction step starting from $n = 0$, until the BBH either merges inside the GC or escapes it. We also refer the reader to Figure 1.

First, we estimate if the BBH will undergo a 2-body merger inside the GC, i.e. merge before the next encounter. For this, we calculate the time between successive binary-single interactions,

t_{bs} , which can be approximated by $\approx 1/(n_s \sigma_{\text{bs}} v_{\text{dis}})$, where n_s is the number density of single BHs, and σ_{bs} is the cross section for a binary-single interaction (e.g., [Samsing et al. 2018b](#)). We then derive the GW-inspiral lifetime of the BBH assuming its eccentricity is $= 0$, t_c , using the prescriptions from [Peters \(1964\)](#). From the two derived time scales, t_{bs} and t_c , we calculate what the minimum eccentricity of the BBH must be for it to undergo a GW merger before the next encounter, i.e. within time t_{bs} , a value we refer to as e_{2b} . Using that the GW lifetime of the BBH can be expressed as $\approx t_c(1 - e^2)^{7/2}$, as derived in [Peters \(1964\)](#) for $e \rightarrow 1$, one now finds that e_{2b} is given approximately by,

$$e_{2b} \approx \sqrt{\left(1 - (t_{\text{bs}}/t_c)^{2/7}\right)}. \quad (3)$$

To now determine if the BBH will actually undergo a 2-body merger inside the GC at this interaction step n , we draw a value for the eccentricity of the BBH, e , assuming a thermal distribution $P(e) = 2e$ ([Heggie 1975](#)). If the drawn eccentricity is $\geq e_{2b}$, the BBH will undergo a 2-body merger, and we record its orbital elements. If the BBH does not merge, i.e. if the drawn eccentricity is $< e_{2b}$, we then move on to estimate if the BBH instead undergoes a merger during its next binary-single interaction.

For estimating the probability of a 3-body merger we use the framework first presented in [Samsing et al. \(2014\)](#), in which the binary-single interaction is pictured as a series of states composed of a binary, referred to as an intermediate state (IMS) binary, and a bound single. As described in [Samsing \(2017\)](#), on average about $N_{\text{IMS}} \approx 20$ IMS binaries will form per binary-single interaction, each with a SMA that is about the initial SMA of the target binary and an eccentricity that is drawn from the thermal distribution $P(e) = 2e$. The probability for a 3-body merger to form during the three-body interaction is equal to the probability for an IMS binary to undergo a GW merger within the orbital time of the bound single. To calculate this probability, we first estimate the characteristic pericentre distance an IMS binary must have for it to undergo a GW capture merger during the interaction, a distance we denote by r_{3b} . Although this distance changes between each IMS in the three-body interaction ([Samsing et al. 2014](#)), one finds that on average r_{3b} is about the distance for which the energy loss through GW emission integrated over one IMS binary orbit is similar to the initial total energy of the three-body system. From this it follows that, $r_{3b} \approx \mathcal{R}_m \times (a/\mathcal{R}_m)^{2/7}$, where \mathcal{R}_m here denotes the Schwarzschild radius of a BH with mass m , and a is the SMA of the target binary, which in our step wise hardening series equals $\delta^n a_{\text{HB}}$ for step n (see [Samsing 2017](#)). The minimum eccentricity of an IMS BBH needed to undergo a GW capture merger during the interaction is then given by,

$$e_{3b} \approx 1 - r_{3b}/a. \quad (4)$$

As for the 2-body mergers, we then draw a value for the IMS BBH eccentricity from the thermal distribution $2e$. We do this up to $N_{\text{IMS}} = 20$ times for each interaction. If one of the drawn eccentricities is $\geq e_{3b}$ a 3-body merger has formed and we save its orbital elements.

If neither a 2-body nor a 3-body merger has formed at the considered step n , we move on to the next SMA step in the hardening series, which after the last binary-single interaction is now $\delta^{n+1} a_{\text{HB}}$, and redo the above calculations. If no merger has formed when the BBH SMA falls below a_{ej} , we assume the BBH escapes the cluster with a SMA = a_{ej} . For this BBH we then calculate what its minimum eccentricity must be for it to merge within in a Hubble time, e_{Ht} .

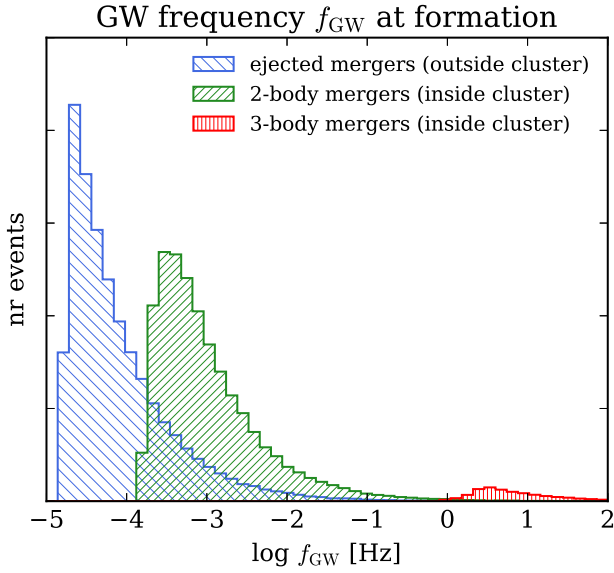


Figure 2. Distribution of GW peak frequency f_{GW} at formation for merging BBHs forming dynamically in GCs. The distributions here are derived using our simple BBH hardening model described in Section 2.1, which combines an MC approach with the analytical framework presented in (Samsing 2017). *Blue:* Distribution of BBHs that are ejected from the GC and merge within a Hubble time (ejected mergers). *Green:* Distribution of BBHs that merge inside the GC *between* their hardening binary-single interactions (2-body mergers). *Red:* Distribution of BBHs that merge inside the GC *during* their hardening binary-single interactions (3-body mergers). The relative contribution from each population depends on the masses of the interacting BHs, the density of single BHs in the GC core, and the escape velocity of the GC; however, all reasonable values lead to about half of all merging BBHs merging inside the cluster (green/red), where about 5% of merging BBHs form in 3-body mergers. We emphasize that the 2-body and 3-body merger populations only can be resolved with GR included in the N -body modeling.

We again draw from a thermal distribution in eccentricity, and if the value is $> e_{\text{Ht}}$ we label the BBH as an ejected BBH merger.

For this paper we follow 10^6 such BBHs starting at their a_{HB} from which we then derive BBH merger fractions, frequency and eccentricity distributions, from the above procedure by going through each of the hardening steps. This allows us to investigate the role of GR effects in what effectively corresponds to $> 10^7$ 2.5 PN binary-single scatterings in just a few seconds. Our results relevant for LISA are described below.

3 ECCENTRIC BLACK HOLE MERGERS IN LISA

The following results are derived using the method described above, applied to the scenario for which the interacting BHs are identical, with a mass $30M_{\odot}$, and for which the population of GCs all have an escape velocity of 50 km s^{-1} (e.g., Harris 1996). We further assume that the number density of single BHs, n_s , in each GC core is 10^5 pc^{-3} . This density is highly uncertain; however, we note that our chosen value results in $\approx 50\%$ of all BBH mergers occurring inside their GC, which is in agreement with the recent PN simulations presented in Rodriguez et al. (2017). For lower values of n_s the relative number of mergers that occur inside the GC increases, and vice versa.

The distributions of peak GW frequency, f_{GW} , at the time of formation of the BBHs that are merging through the three dif-

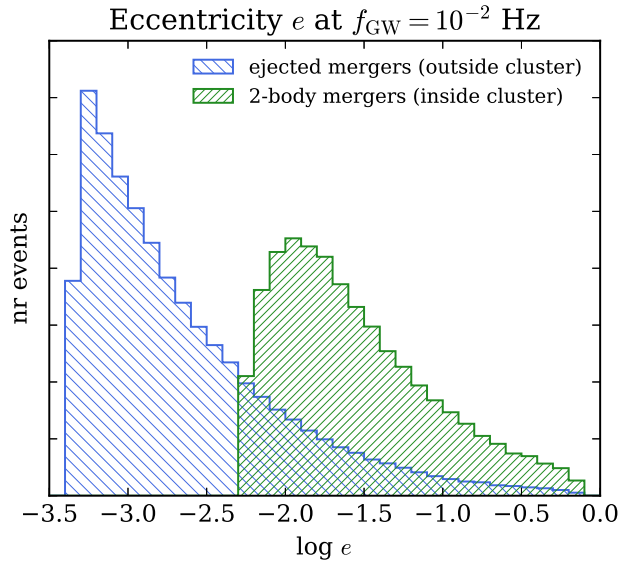


Figure 3. Distribution of BBH orbital eccentricity e at 10^{-2} Hz derived using all the BBH mergers from the set presented in Figure 2 that have an initial $f_{\text{GW}} < 10^{-2}$ Hz. As the 3-body mergers peak at much higher frequencies, the considered set is completely dominated by the ejected (blue) and 2-body (green) mergers. As seen, the 2-body mergers dominate the fraction that will have a resolvable eccentricity (> 0.01) in the LISA band (10^{-2} Hz). This population will therefore play a key role in determining the origin of BBH mergers using a LISA-like instrument, as, e.g., field BBHs are expected to be circular to a much higher degree in LISA.

ferent pathways considered in this work (ejected merger, 2-body merger, 3-body merger) are shown in Figure 2. For this we used the approximation $f_{\text{GW}} = \pi^{-1} \sqrt{2Gm/r_p^3}$, where r_p is the pericentre distance at the time of formation of the merging BBH (e.g., Wen 2003; Samsing 2017). The ejected mergers (blue) initially distribute at relatively low f_{GW} with a peak between $10^{-5} - 10^{-4}$ Hz, and will therefore drift through both LISA and LIGO. The possibility for joint observations have been suggested for such a population (e.g., Sesana 2016; Seto 2016). The 3-body mergers (red) all have a much higher initial f_{GW} with a peak between $10^0 - 10^1$ Hz, and will therefore elude the LISA band and form directly in the proposed DECIGO (Kawamura et al. 2011; Isoyama et al. 2018)/Tian Qin (Luo et al. 2016) band before entering the LIGO band (e.g., Chen & Amaro-Seoane 2017; Samsing et al. 2018a). We note here that these two distributions are in full agreement with those found in Samsing et al. (2018a), in which the distributions were resolved using full numerical 2.5 PN scatterings using data from the MOCCA code (Giersz et al. 2013; Askar et al. 2017). This validates at least this part of our framework. The 2-body mergers (green) interestingly distribute between the ejected and the 3-body mergers, with a peak only slightly below the maximum sensitivity region of LISA. A proper understanding and modeling of this population is required for using LISA to determine the origin of BBH mergers. As stated in Section 2, we note that this population has not been studied in this context before. In Paper II of this series we investigate in detail the GW signatures of these three dynamically formed populations in the LISA band.

The eccentricity distribution of the BBH mergers evaluated at 10^{-2} Hz, near the peak of the LISA sensitivity, is shown in Figure 3. To derive this distribution, we use the evolution equations from Peters (1964) to propagate the initial BBH eccentricity distribu-

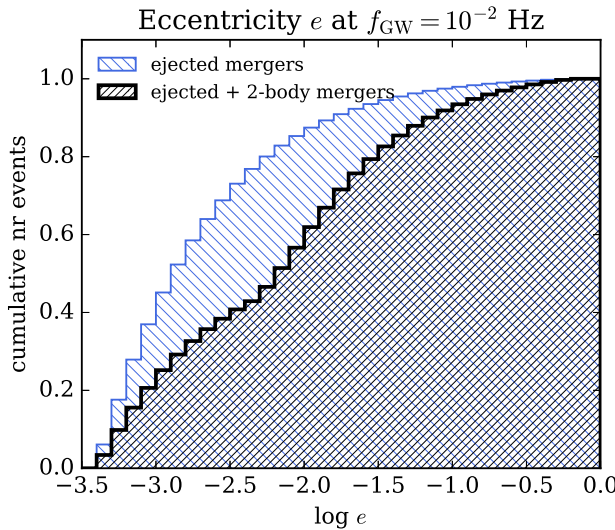


Figure 4. Cumulative distribution of the eccentricity distributions shown in Figure 3. When the 2-body mergers are included (black), $\approx 40\%$ of merging BBHs will have an eccentricity > 0.01 at 10^{-2} Hz, near the peak sensitivity of the LISA band. We note that this fraction is about 4 times higher than recently reported by (Breivik et al. 2016), who effectively only considered the ejected population. A substantial fraction of eccentric BBH mergers are therefore expected in LISA if the dynamical GC channel contributes to the BBH merger rate. This finding should be taken into account when optimizing science cases and instrumental designs.

tion, with initial peak GW frequency $f_{\text{GW}} < 10^{-2}$ Hz, to the value at $f_{\text{GW}} = 10^{-2}$ Hz. As seen, the 2-body mergers, i.e. the BBHs that merge between encounters inside the GC, completely dominate the fraction of mergers that will have an eccentricity resolvable by LISA ($e > 0.01$). To clarify this statement, Figure 4 shows the corresponding cumulative distribution. As seen, if only the ejected mergers are considered (as was effectively done in Breivik et al. (2016)), then only $\approx 10\%$ will have an eccentricity > 0.01 at 10^{-2} Hz (blue); however, when the 2-body mergers are included $\approx 40\%$ of all the mergers will have an eccentricity > 0.01 (black). This is an important correction, as some recent studies have argued that eccentric populations would hint for BBH mergers forming near massive BHs (e.g., Nishizawa et al. 2017). Our results show that GCs can produce eccentric mergers in LISA as well, greatly motivating further and more detailed studies on systems.

From this we conclude that BBH mergers forming in GCs are expected to lead to a notable distribution of eccentric sources (> 0.01) in the LISA band (10^{-2} Hz), with a relative fraction that is significantly higher than recently reported by Breivik et al. (2016). This not only shows the importance of a proper inclusion of GR terms in current N -body studies, but also the bright prospects of observationally distinguishing where and how BBH mergers form in our Universe with LISA.

4 CONCLUSIONS

In Paper I of this series, we have explored the role of GR effects in the dynamical evolution of BBHs inside GCs, and found that the population that merges through GW emission between their hardening binary-single interactions, referred to as 2-body mergers, all appear with a notable eccentricity (> 0.01) in the LISA band

(10^{-2} Hz). Using a simple MC approach together with the analytical framework presented in Samsing (2017), we find that with the inclusion of these 2-body mergers, $\approx 40\%$ of all BBH mergers from GCs will be eccentric in LISA, which is ≈ 4 times more than recently stated by Breivik et al. (2016), in which only Newtonian gravity was included.

That GCs are expected to have much richer distributions in eccentricity across the LISA band than previously thought, has important implications for how to observationally distinguish BBH merger channels from each other using LISA, as well as LIGO (e.g., Nishizawa et al. 2016; Breivik et al. 2016; Nishizawa et al. 2017; Samsing et al. 2018a). The reason is that different channels will have different eccentricity distributions, e.g. isolated field binaries are believed to have almost circularized once entering LISA, whereas BBH mergers assembled near massive black holes have been shown to have a notable eccentricity in LISA (e.g., Nishizawa et al. 2017).

Our results likewise indicate that the background of unresolved sources observable by LISA, is likely to have a significant fraction of eccentric sources. Including such a population will lead to changes in the expected background spectrum, which often is assumed to be dominated by circular BBHs partly due to the Newtonian results derived in Rodriguez et al. (2016a), that we argue greatly underestimates the true fraction of eccentric sources. In Paper II of this series, we explore the tracks of individually resolvable, eccentric BBHs through the LISA band as well as the effect of unresolvable eccentric systems on the gravitational wave background detectable by LISA, each a result of the GR effects discussed in this paper.

ACKNOWLEDGEMENTS

It is a pleasure to thank M. Giersz, A. Askar, E. Kovetz, and M. Kamionkowski for helpful discussions. J.S. acknowledges support from the Lyman Spitzer Fellowship. D.J.D. acknowledges financial support from NASA through Einstein Postdoctoral Fellowship award number PF6-170151. D.J.D. also thanks Adrian Price-Whelan and Lauren Glattly for their hospitality during the conception of this work.

References

- Aarseth S. J., Heggie D. C., 1976, *A&A*, **53**, 259
- Abbott B. P., et al., 2016a, *Physical Review X*, **6**, 041015
- Abbott B. P., et al., 2016b, *Physical Review Letters*, **116**, 061102
- Abbott B. P., et al., 2016c, *Physical Review Letters*, **116**, 241103
- Abbott B. P., et al., 2017a, *Physical Review Letters*, **118**, 221101
- Abbott B. P., et al., 2017b, *Physical Review Letters*, **119**, 141101
- Amaro-Seoane P., et al., 2017, preprint, ([arXiv:1702.00786](https://arxiv.org/abs/1702.00786))
- Antonini F., Rasio F. A., 2016, *ApJ*, **831**, 187
- Antonini F., Rodriguez C. L., Petrovich C., Fischer C. L., 2017, preprint, ([arXiv:1711.07142](https://arxiv.org/abs/1711.07142))
- Askar A., Szkudlarek M., Gondek-Rosińska D., Giersz M., Bulik T., 2017, *MNRAS*, **464**, L36
- Bae Y.-B., Kim C., Lee H. M., 2014, *MNRAS*, **440**, 2714
- Banerjee S., Baumgardt H., Kroupa P., 2010, *MNRAS*, **402**, 371
- Bartos I., Kocsis B., Haiman Z., Márka S., 2017, *ApJ*, **835**, 165
- Belczynski K., Holz D. E., Bulik T., O’Shaughnessy R., 2016a, *Nature*, **534**, 512
- Belczynski K., Repetto S., Holz D. E., O’Shaughnessy R., Bulik T., Berti E., Fryer C., Dominik M., 2016b, *ApJ*, **819**, 108
- Bird S., Cholis I., Muñoz J. B., Ali-Haïmoud Y., Kamionkowski M., Kovetz E. D., Raccanelli A., Riess A. G., 2016, *Physical Review Letters*, **116**, 201301

6 *Samsing, D’Orazio*

Blanchet L., 2014, *Living Reviews in Relativity*, 17

Breivik K., Rodriguez C. L., Larson S. L., Kalogera V., Rasio F. A., 2016, *ApJL*, 830, L18

Carr B., Kühnel F., Sandstad M., 2016, *PRD*, 94, 083504

Chen X., Amaro-Seoane P., 2017, *ApJL*, 842, L2

Cholis I., Kovetz E. D., Ali-Haïmoud Y., Bird S., Kamionkowski M., Muñoz J. B., Raccanelli A., 2016, *PRD*, 94, 084013

D’Orazio D. J., Loeb A., 2017, preprint, ([arXiv:1706.04211](https://arxiv.org/abs/1706.04211))

Dominik M., Belczynski K., Fryer C., Holz D. E., Berti E., Bulik T., Mandel I., O’Shaughnessy R., 2012, *ApJ*, 759, 52

Dominik M., Belczynski K., Fryer C., Holz D. E., Berti E., Bulik T., Mandel I., O’Shaughnessy R., 2013, *ApJ*, 779, 72

Dominik M., et al., 2015, *ApJ*, 806, 263

Giersz M., Heggie D. C., Hurley J. R., Hypki A., 2013, *MNRAS*, 431, 2184

Gültekin K., Miller M. C., Hamilton D. P., 2006, *ApJ*, 640, 156

Harris W. E., 1996, *AJ*, 112, 1487

Heggie D. C., 1975, *MNRAS*, 173, 729

Hoang B.-M., Naoz S., Kocsis B., Rasio F. A., Dosopoulou F., 2017, preprint, ([arXiv:1706.09896](https://arxiv.org/abs/1706.09896))

Hong J., Lee H. M., 2015, *MNRAS*, 448, 754

Hut P., Bahcall J. N., 1983, *ApJ*, 268, 319

Isoyama S., Nakano H., Nakamura T., 2018, preprint, ([arXiv:1802.06977](https://arxiv.org/abs/1802.06977))

Janiuk A., Bejger M., Charzyński S., Sukova P., 2017, preprint, 51, 7 ([arXiv:1604.07132](https://arxiv.org/abs/1604.07132))

Kawamura S., et al., 2011, *Classical and Quantum Gravity*, 28, 094011

Liu B., Lai D., 2017, *ApJL*, 846, L11

Loeb A., 2016, *ApJL*, 819, L21

Luo J., et al., 2016, *Classical and Quantum Gravity*, 33, 035010

McKernan B., et al., 2017, preprint, ([arXiv:1702.07818](https://arxiv.org/abs/1702.07818))

Nishizawa A., Berti E., Klein A., Sesana A., 2016, *PRD*, 94, 064020

Nishizawa A., Sesana A., Berti E., Klein A., 2017, *MNRAS*, 465, 4375

O’Leary R. M., Kocsis B., Loeb A., 2009, *MNRAS*, 395, 2127

Park D., Kim C., Lee H. M., Bae Y.-B., Belczynski K., 2017, *MNRAS*, 469, 4665

Peters P., 1964, *Phys. Rev.*, 136, B1224

Portegies Zwart S. F., McMillan S. L. W., 2000, *ApJL*, 528, L17

Rodriguez C. L., Morscher M., Patabiraman B., Chatterjee S., Haster C.-J., Rasio F. A., 2015, *Physical Review Letters*, 115, 051101

Rodriguez C. L., Chatterjee S., Rasio F. A., 2016a, *PRD*, 93, 084029

Rodriguez C. L., Haster C.-J., Chatterjee S., Kalogera V., Rasio F. A., 2016b, *ApJL*, 824, L8

Rodriguez C. L., Zevin M., Pankow C., Kalogera V., Rasio F. A., 2016c, *ApJL*, 832, L2

Rodriguez C. L., Amaro-Seoane P., Chatterjee S., Rasio F. A., 2017, preprint, ([arXiv:1712.04937](https://arxiv.org/abs/1712.04937))

Samsing J., 2017, preprint, ([arXiv:1711.07452](https://arxiv.org/abs/1711.07452))

Samsing J., MacLeod M., Ramirez-Ruiz E., 2014, *ApJ*, 784, 71

Samsing J., D’Orazio D. J., Askar A., Giersz M., 2018a, preprint, ([arXiv:1802.08654](https://arxiv.org/abs/1802.08654))

Samsing J., MacLeod M., Ramirez-Ruiz E., 2018b, *ApJ*, 853, 140

Samsing J., Askar A., Giersz M., 2018c, *ApJ*, 855, 124

Sasaki M., Suyama T., Tanaka T., Yokoyama S., 2016, *Physical Review Letters*, 117, 061101

Sesana A., 2016, *Physical Review Letters*, 116, 231102

Seto N., 2016, *MNRAS*, 460, L1

Stone N. C., Metzger B. D., Haiman Z., 2017, *MNRAS*, 464, 946

Tanikawa A., 2013, *MNRAS*, 435, 1358

VanLandingham J. H., Miller M. C., Hamilton D. P., Richardson D. C., 2016, *ApJ*, 828, 77

Wen L., 2003, *ApJ*, 598, 419

Woosley S. E., 2016, *ApJL*, 824, L10